Slim P E hysteresis loop and anomalous dielectric response in sol-gel derived antiferroelectric Pb Zr O 3 thin films

Jayanta Parui and S. B. Krupanidhi

Citation: Journal of Applied Physics **104**, 024107 (2008); doi: 10.1063/1.2956695
View online: http://dx.doi.org/10.1063/1.2956695
View Table of Contents: http://scitation.aip.org/content/aip/journal/jap/104/2?ver=pdfcov
Published by the AIP Publishing

Slim *P-E* hysteresis loop and anomalous dielectric response in sol-gel derived antiferroelectric $PbZrO_3$ thin films

Jayanta Parui and S. B. Krupanidhi[a)]
Materials Research Centre, Indian Institute of Science, Bangalore-560012, India

(Received 27 December 2007; accepted 13 May 2008; published online 21 July 2008)

Sol-gel derived $PbZrO_3$ (PZ) thin films have been deposited on $Pt(111)/Ti/SiO_2/Si$ substrate and according to the pseudotetragonal symmetry of PZ, the relatively preferred $(110)_t$ oriented phase formation has been noticed. The room temperature *P-E* hysteresis loops have been observed to be slim by nature. The slim hysteresis loops are attributed to the $[110]_t$ directional antiparallel lattice motion of Pb ions and by the directionality of the applied electric field. Pure PZ formation has been characterized by the dielectric phase transition at 235 °C and antiferroelectric *P-E* hysteresis loops at room temperature. Dielectric response has been characterized within a frequency domain of 100 Hz–1 MHz at various temperatures ranging from 40 to 350 °C. Though frequency dispersion of dielectric behaves like a Maxwell–Wagner type of relaxation, ω^2 dependency of ac conductivity indicates that there must be *G-C* equivalent circuit dominance at high frequency. The presence of trap charges in PZ has been determined by Arrhenius plots of ac conductivity. The temperature dependent n (calculated from the universal power law of ac conductivity) values indicate an anomalous behavior of the trapped charges. This anomaly has been explained by strongly and weakly correlated potential wells of trapped charges and their behavior on thermal activation. The dominance of circuit/circuits resembling Maxwell–Wagner type has been investigated by logarithmic Nyquist plots at various temperatures and it has been justified that the dielectric dispersion is not from the actual Maxwell–Wagner-type response. © *2008 American Institute of Physics*. [DOI: 10.1063/1.2956695]

I. INTRODUCTION

Antiferroelectric (AFE) thin films have been extensively studied for their potential application for integrated circuit devices through the combination with silicon micromachining technology for sensors and actuators.[1,2] In recent years, the giant electrocaloric effect of AFE lead zirconate titanate (PZT) has been investigated and it has been recognized as a potential candidate for electrical refrigeration devices.[3] Among the three ways to microelectromachining (MEM), electrical phase switching of AFEs is well recognized in PZ and Sn modified PZT (PZST) for MEM applications.[4,5] The other two ways to MEM are piezoelectricity and electrostriction.[5] PZT is well recognized for its piezoelectric property[6] and relaxor ferroelectric (FE) materials, such as La-modified PZT (PLZT) (Ref. 7) and lead magnesium niobate,[8] have been categorized as electrostrictive materials. In the case of electric field induced strain generation, PZST is the more familiar material to produce large transformational strain of ~1% and hence it is widely suggested for high force actuators.[5,9,10] However, the stoichiometric complexity and possibility of structural inhomogeneity in PZST lead to study of relatively simple materials such as PZ. From the crystallographic point of view, the orthorhombic AFE phase of PZ consists of eight tetragonal primitive perovskite cells[11] and each tetragonal primitive cell has antipolar dipoles along the $[110]_t$ (t stands for the convention of tetragonal primitive perovskite cell of PZ) direction.[12] Therefore from the point of polarization hysteresis and dielectric property, $(110)_t$ oriented PZ thin films are expected to have different properties compared to $(111)_t$ and $(100)_t$ oriented PZ thin films. However, Tani *et al.*[13] already investigated the $(111)_t$ and $(100)_t$ oriented sol-gel grown PZ thin films and they found a noticeable difference in electrical properties on the basis of crystallographic orientations. In this paper, we have compared the results of relatively $(110)_t$ oriented thin films to other reports on the basis of the crystallographic orientations and thicknesses.[13–15] According to the comparison, we have concluded that slim *P-E* hysteresis loops of PZ thin films are because of the relatively preferred $(110)_t$ crystallographic orientation.

Solid thin films have many aspects to determine the true response of the sample. Among them, the Nyquist plot, ac conductivity, and Arrhenius plot of ac conductivity are recognized to be the most important characterization techniques to deal with.[16] Though in our earlier paper, we have discussed a few aspects of $(110)_t$ oriented PZ thin films grown by polymer modified sol-gel route,[17] here in this paper we have discussed differently grown relatively $(110)_t$ oriented PZ thin films by dielectric dispersion, Nyquist plot, and detailed analysis of ac conductivity. Other characterizations such as x-ray diffraction (XRD), electrical phase transition, and dielectric phase transition have also been reported here as its primary characterizations. Apart from them, here we have presented the *P-E* hysteresis loops with better accuracy and at virtual ground mode, and dielectric response has been explained at a relatively higher frequency range.

a)Author to whom correspondence should be addressed. Electronic mail: sbk@mrc.iisc.ernet.in.

II. EXPERIMENTAL PROCEDURES

Solution of PZ has been prepared by polyvinylpyrrolidone modified sol-gel technique.[17] This 0.3*M* solution has been deposited on $Pt(111)/Ti/SiO_2/Si$ substrate by spin coating at 3500 rpm for 30 s. Single coated films have been pyrolyzed at 350 °C for 5 min followed by an annealing at temperature of 750 °C for 30 min in an oxygen rich environment. The same solution has been coated five times on the single coated annealed substrate at the same spinning parameters followed by the same heat treatment to pyrolyze on and after each coating. The five times coated pyrolyzed film has also been crystallized on the same annealing treatment as described for single coating. The crystallinity of the films has been determined at room temperature by XRD (Scintag 3100) and the film thicknesses have been measured by cross section scanning electron microscopy (SEM). The total thickness is measured as ~0.68 μm. For electrical characterization, one corner of the films has been etched out by HF solution to expose the Pt bottom layer, which has been used as bottom electrode. Gold dots of area of 1.963×10^{-3} cm^2 have been deposited on the films by e-beam evaporation technique and shadow masking. The gold dots, deposited for top electrodes, have been annealed at 320 °C for 20 min for Ohmic contact. Weak-field dielectric measurements have been performed by Agilent Precision impedance analyzer 4294A and Keithley 3330 *LCZ* meter. Measurements have been taken from 100 Hz to 1 MHz at an oscillation voltage of 500 mV. *P-E* hysteresis measurement has been performed at 1 kHz using Precision Workstation materials analyzer (Radiant Technologies, Inc.) in virtual ground mode at room temperature. Temperature varied measurements have been performed on a potential-integral-differential controlled heater slab kept in a closed box.

III. RESULTS AND DISCUSSION

A. X-ray diffraction and polarization hysteresis

In Fig. 1, we have presented an XRD pattern of PZ thin films based on tetragonal primitive perovskite cell consideration.[14] The intensity of XRD has been plotted in log scale and it has been seen that the film is preferably $(110)_t$ oriented and according to JCPDS-ICDD index 75-1607, it is preferably $(122)_O$ oriented, where *O* stands for orthorhombic symmetry. However, from this XRD [Fig. 1(a)] it has been noticed that there is a small hump from ~23° to the $(110)_t$ peak. This may be because of pyrochlore phase formation due to possible lead loss at the time of single layer annealing. The same hump has also been seen in the XRD of single layer PZ [Fig. 1(b)]. Along with $(110)_t$ and $(202)_t$, a small peak at 2θ=55.62° has been observed, which is found to be undetermined according to the tetragonal symmetry as well as orthorhombic symmetry of PZ. However, it is well known that the formation of Pt_3Pb alloy at the interface is the deterministic phenomenon for (111) oriented PZT thin films.[18,19] This formation of Pt_3Pb alloy can be expected for any Pb based perovskite thin films deposited on Pt coated substrates. In our present study, the formation of $(110)_t$ oriented PZ is assumed to be due to the formation of Pt_3Pb at the interface and applied annealing temperature and time.[18,19] The assumption is based on the lattice constant of Pt_3Pb (a=4.05 Å,) which leads to a lattice mismatch of 2.7% according to the tetragonal symmetry of PZ (for the tetragonal symmetry of PZ, a=4.15 Å, b=4.15 Å, and c=4.10 Å and for the orthorhombic structure PZ, a=5.87 Å, b=11.74 Å, and c=8.20 Å).[4,17] Moreover, as the annealing temperature and time are suitable for Pt_3Pb alloy formation[18,19] and as the lattice mismatch between PZ and Pt_3Pb alloy is lesser than that between PZ and Pt (a=3.923 Å), we can say that the plausible reason for the relatively preferred orientation of PZ thin films is the combined effect of annealing temperature and time along with the formation of Pt_3Pb alloy.

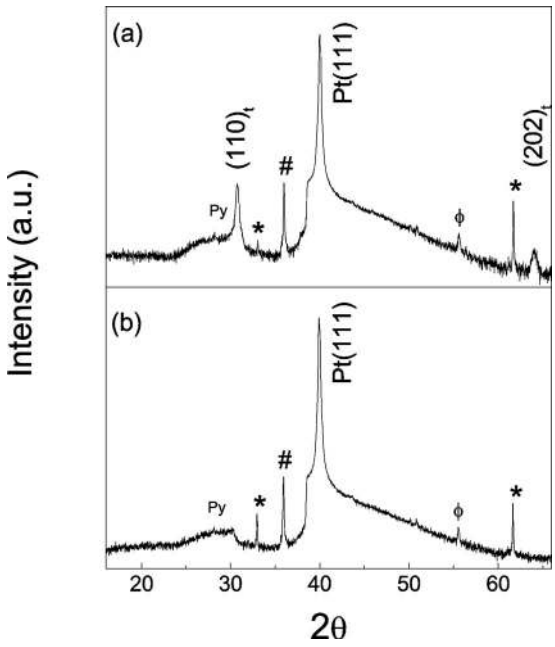

FIG. 1. (XRD) pattern of sol-gel grown crystalline $PbZrO_3$ (PZ) thin films on $Pt(111)/Ti/SiO_2/Si$ substrate. (a) XRD of ~0.68 μm thick films after final annealing and (b) XRD of single coated PZ thin films after annealing at 750 °C. Py, *, #, and ϕ denote the possible pyrochlore phase, undetermined Si peak, Pt K_β peak, and an undetermined peak of crystalline PZ thin film, respectively.

For the *P-E* hysteresis measurements, the direction of the applied electric field can be assumed to be parallel to the film orientation, which means that the applied electric field is normal to the $(110)_t$ planes of PZ thin films. According to Jona *et al.*,[12] antipolar dipoles of PZ are along the $[110]_t$ direction of its tetragonal primitive cells. Shebanov *et al.*[20] showed that on application of electric field, the antipolar dipoles can be oriented to a polar direction with an increase in unit cell volume by 0.35 Å^3 due to field induced phase transition. After the alignment of the dipoles, the tetragonal unit cells become rhombohedral and PZ acts as a FE at that particular applied electric field. This rhombohedral phase has a crystallographic angle α_{rh} (α_{rh}=89.8° or 89.95°) (Ref. 10) just less than 90° and this phase exhibits FE polarization along the $[111]_t$ direction.[20,21] Hence, we can visualize that the crystallographic angle of the tetragonal unit cell, α_{tet} (α_{tet}=90°) just gets transformed to α_{rh} on field induced phase transformation. The small deviation of the crystallographic angle of the rhombohedral unit cell from that of the tetragonal unit cell ($\alpha_{rh} \approx 90° = \alpha_{tet}$) indicates that after phase

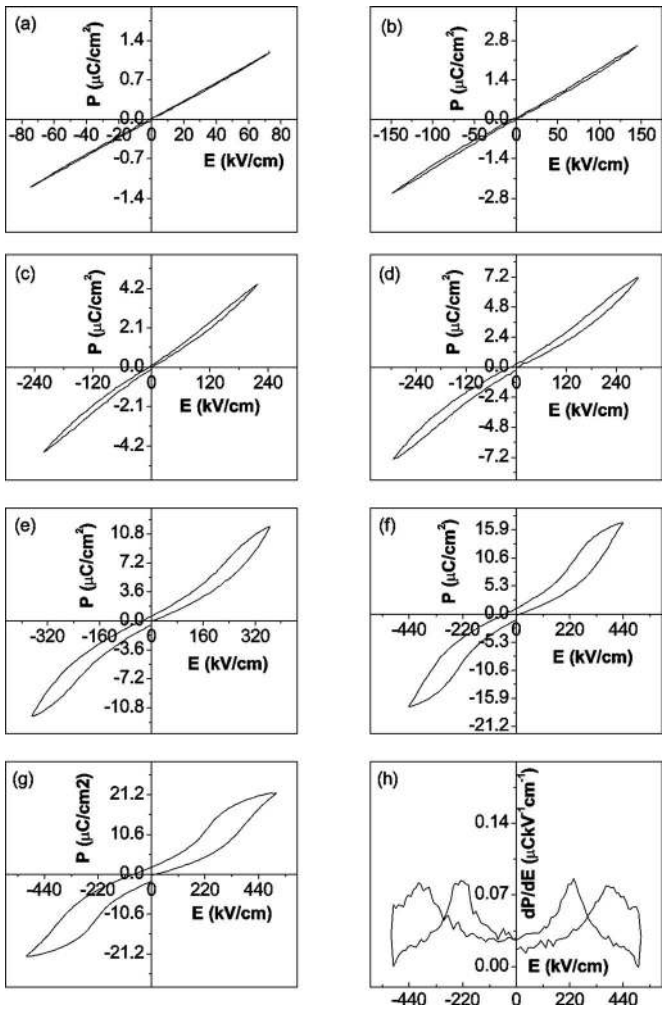

FIG. 2. Room temperature *P-E* hysteresis loops at various applied fields (or various voltages) measured at 1 kHz. (a)-(g) depict *P-E* hysteresis loops at different voltage drives from 5 to 35 V, respectively. (f) is the differentiation of the *P-E* hysteresis loop to determine field induced phase switching windows at 35 V drive and the phase switching windows at that voltage drive are 134 kV/cm at positive drive and 174 kV/cm at negative drive.

transformation, the direction of the applied electric field remains almost the same.[20] Hence, the applied electric field along the $[110]_t$ direction of the rhombohedral unit cell will sense the polarization along the $(110)_t$ direction, whereas the expected better FE polarization direction of this rhombohedral is along the $[111]_t$ direction.[20,21] Therefore, according to the lattice motion of the oxygen framework, polarization along the $[110]_t$ direction is assumed to be lesser than that along the $[111]_t$ direction[12] and according to the crystallographic point of view, the polarization response along the $[110]_t$ direction is just a vectorial component of the response along the $[111]_t$ direction of the rhombohedral.[5] Thus, the polarization and polarization hysteresis of $(110)_t$ oriented PZ films are expected to be small and slim by nature, respectively. The room temperature *P-E* hysteresis loops have been measured at 1 kHz and at various applied electric fields (or various voltages) and according to Fesenko *et al.*,[22] these loops are supposed to show "sixfold" hysteresis loops above an applied field of 500 kV/cm. However, the room temperature *P-E* hysteresis loops, presented in Fig. 2, show that only "twofold" hysteresis loops have been observed though the maximum applied field is higher than 500 kV/cm. However, the presence of residual stress in the thin film form of PZ can be attributed to mask the many fold hysteresis loops within this range of applied electric field. Thus only twofold hysteresis loops have been noticed in the present measurement of *P-E* hysteresis loops. Among these hysteresis loops, polarization saturation has been observed at 513 kV/cm with the maximum polarization value of $\sim 21.6\ \mu C/cm^2$ [Fig. 2(g)] and the forward AFE to FE transition has been observed at ~370 kV/cm, whereas reverse transition has been observed at ~236 kV/cm [Fig. 2(h)]. Thus, the difference between forward and reverse transitions has been observed only to be 134 kV/cm, which is very small to show a slim hysteresis loop. On the other hand, AFE to FE transition at negative field drive has been observed at ~−401 kV/cm, whereas FE to AFE has been noticed at ~−227 kV/cm. At this negative field drive, the difference between the reverse and forward transitions has been noticed only to be 174 kV/cm. This difference may be due to difference in electrodes, where the bottom electrode is Pt and the top electrode is Au. The influence of an unsymmetrical electrode may have an influence on the polarization values at different voltage drives. It has been seen that at the negative voltage drive, the maximum polarization is $\sim 21.8\ \mu C/cm^2$. Therefore, it can be said that the different electrodes have a prominent effect on field induced phase switching, whereas their influence on polarization values is not very distinguishable. According to Zhai *et al.*,[14] a decrease in film thickness leads to an increase in the switching field of AFE-FE phase transitions in both the directions. According to their report, $(001)_t$ oriented 900 nm thick film on $LaNiO_3$ buffer layer has showed that the difference between the forward and reverse transitions is 270 kV/cm, whereas a recent observation by Alkoy *et al.*[15] an 180 nm thick $(111)_t$ oriented PZ film has the forward switching field at 350 kV/cm and reverse one at 200 kV/cm, leading to a difference of only 150 kV/cm. Therefore, the switching field of PZ depends on both preferred orientation and thickness. Though the difference in switching field in negative voltage drive is more than 150 kV/cm, the difference in positive voltage drive is less than it. On the other hand, both the differences are less than what was reported by Zhai *et al.*[14] for a 900 nm thick film. Despite of that, the thickness of the present film (~0.68 μm) is less than 900 nm and it should show a relatively greater difference of switching fields.[14] However, though a comparative study of $(100)_t$ and $(111)_t$ oriented PZ films was reported by Tani *et al.*,[13] only coercive field was mentioned for highly $(111)_t$ oriented films, whereas in their report, there is no note on the difference between forward and reverse phase switchings. Moreover, most of the $(100)_t$ or $(111)_t$ oriented PZ films have been prepared on buffer layers, such as $LaNiO_3$ (Ref. 14) or TiO_2,[13] and without buffer layers, sol-gel grown PZ thin films on $Pt(111)/Ti/SiO_2/Si$ have ended up with either $(111)_t$ or $(100)_t$ orientation.[13,15,23] In our study, we have not used any buffer layer to stabilize $(110)_t$ phase and thus growth kinetics of PZ films is completely different from earlier reports. However, we have got relatively slimmer hysteresis loops because of the highly $(110)_t$ orientation and it is supported by the switching mechanism of AFE-FE transition

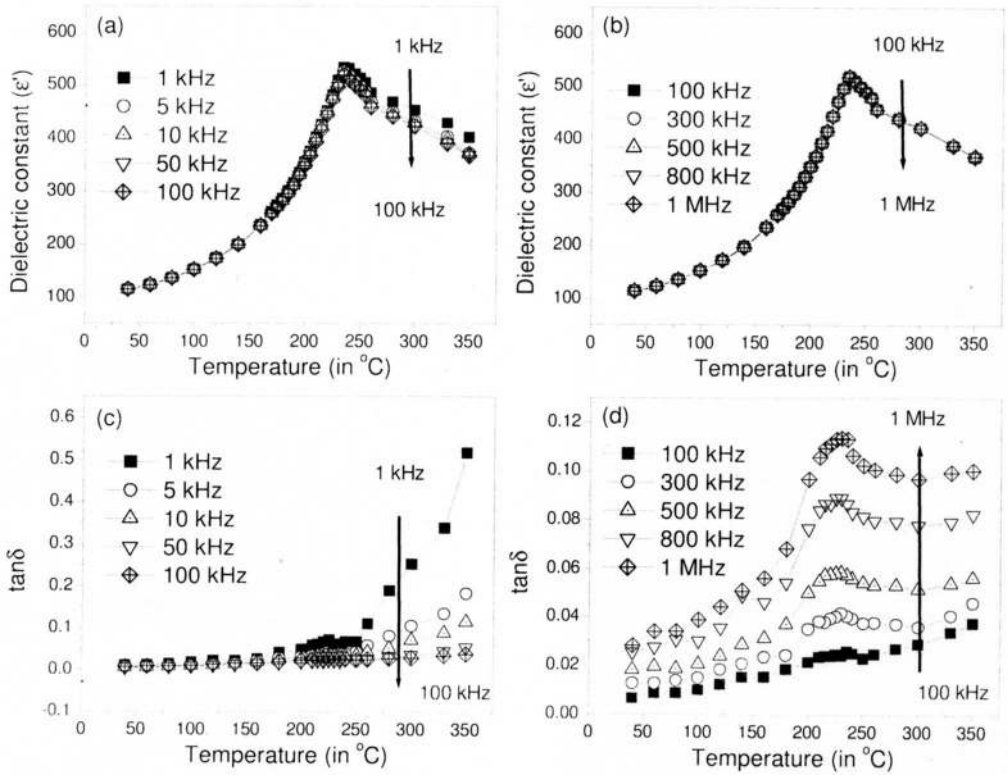

FIG. 3. (a) Dielectric phase transition of PZ thin film within the frequency range of 1–100 kHz and (b) within the frequency range of 100 kHz–1 MHz. (c) Phase transition of tan δ within the frequency range of 1–100 kHz and (d) within 100 kHz–1 MHz.

as reported by Jona *et al.*[12] Moreover, prepared $(110)_t$ preferred oriented PZ thin films of ~0.68 μm thickness have ~2 $\mu C/cm^2$ remnant polarization on 513 kV/cm voltage drive, which is the signature of the possible FE nature of predeposited single layer of PZ as the thickness of this single layer is very thin (~100 nm).[23–25]

B. Dielectric dispersion and dielectric phase transition

In Fig. 3, we have presented a dielectric phase transition of $(110)_t$ oriented PZ thin films. Figures 3(a) and 3(b) show the dielectric phase transition within the frequency ranges of 1–100 kHz and 100 kHz–1 MHz, respectively. Within the entire frequency range from 1 kHz to 1 MHz, the phase transition is observed at 235 °C. The peak value of the dielectric constant is 518 at 100 kHz and the room temperature dielectric constant is 114 at the same frequency. This small difference between the room temperature dielectric constant and dielectric constant at its peak value may have arouse from the possible pyrochlore phase formation due to Pb loss during annealing (Fig. 1). However, the phase transition at 235 °C is one of the confirmations of pure PZ formation.[4] Figure 3(c) shows the temperature dependence of tan δ within the frequency range of 1–100 kHz, whereas Fig. 3(d) presents the temperature dependence of tan δ within the frequency range of 100 kHz–1 MHz. From Fig. 3(c), it can be noticed that at low frequency, such as below 100 kHz, no phase transition in tan δ has been observed. This absence of phase transition can be attributed to the hopping charge contribution for the masking of the true dielectric nature of PZ. For this reason an investigation in a relatively high frequency region [Fig. 3(d)] has revealed a clear phase transition in tan δ versus temperature at 235 °C. This phenomenon indicates that the true dielectric nature of PZ thin films has not been masked by hopping charge contribution in the high frequency region. However, from the phase transition plots of tan δ [Fig. 3(d)], it has been noticed that there is a slight increasing trend of tan δ values at the higher temperature region than the phase transition temperature. This slight increase in tan δ values indicates that though hopping charge contribution at the high frequency region is unable to mask the phase transition of tan δ, it can be dominating at higher temperatures.

Apart from the thermal phase transition, dielectric response with respect to frequency has been presented in Fig. 4. The real and imaginary parts of the dielectric constants have been presented separately in Figs. 4(a) and 4(b), respectively. From the frequency dispersion of the real part of the dielectric constant [Fig. 4(a)], it has been observed that there is almost no frequency dispersion at the low temperature region (up to 180 °C), whereas at the high temperature region (above 180–350 °C), relatively strong dielectric dispersion has been noticed. However, on the increase in temperature it has been observed that the dielectric dispersion extends to higher frequencies [Fig. 4(a)]. This phenomenon indicates that on the increase in temperature, hopping charge starts dominating on the higher frequency region. In general, hopping charge dominance is observed in the low frequency region, masking the true property of the materials.[26,27] Moreover, very strong frequency dispersion in the imaginary part

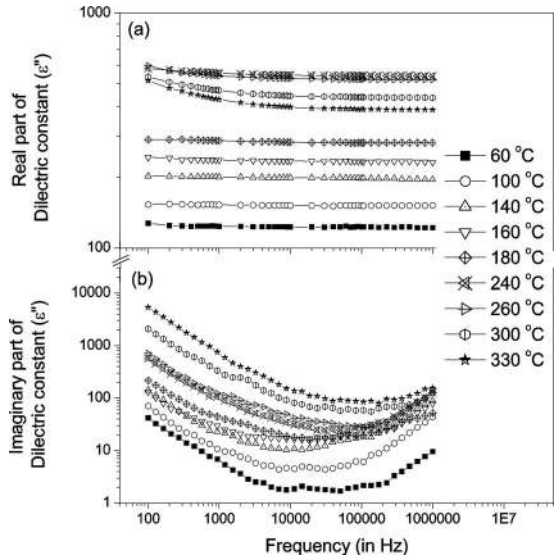

FIG. 4. Frequency dispersion of the real part of the dielectric constant and (b) the imaginary part of the dielectric constants. The dominance of hopping charge is prominent at high temperatures.

of the dielectric constant has been observed with a little increase in values at the extremely high frequency region of measurement [Fig. 4(b)]. Such a phenomenon indicates a Maxwell-Wagner type of dielectric response.[16] The presentations of the real part of the dielectric constants along with the imaginary part of the dielectric constants in Fig. 5 show the possible presence of the Maxwell-Wagner type of dielectric dispersion. From the dielectric dispersions of the real and imaginary parts at 60, 200, and 330 °C [Figs. 5(a)–5(c), respectively], it can be predicted that measurement of dielectric response is below the loss peak frequency. According to the Maxwell-Wagner-type dielectric response, at the low frequency region, the real part of the dielectric constant should be frequency independent. However, in the present study, the presence of hopping charge carriers shows prominent low frequency dispersion in the real part of the dielectric constant. According to the Kramers-Kronig relation

$$\chi'(0) = \varepsilon'(0) - 1 = \frac{2}{\pi}\int_{-\infty}^{\infty} \chi''(\omega) d \ln(\omega), \tag{1}$$

any abrupt change in dielectric constant is accompanied by a peak in the dielectric loss.[28] In the equation, $\chi'(\omega)$ represents the real part and $\chi''(\omega)$ represents the imaginary part of the frequency dependent complex dielectric response. For a FE or AFE material, the value of ε is normally larger than unity and therefore the representations in terms of either ε or χ are synonymous. However, in our present study, measurements are below the loss peak frequency and there is no abrupt change in the dielectric constant in the real part. So the dielectric dispersion is not loss peak accompanied. In general, dc conduction in dielectric solid does not affect the real part of the dielectric constant as it does not change the relative distance between the centers of opposite charges. Therefore, there must be some interaction between hopping charge conduction and dielectric polarization in the samples under study. It is reported that hopping charge conduction originates from trapped charge in dielectric solids.[16] The trapped

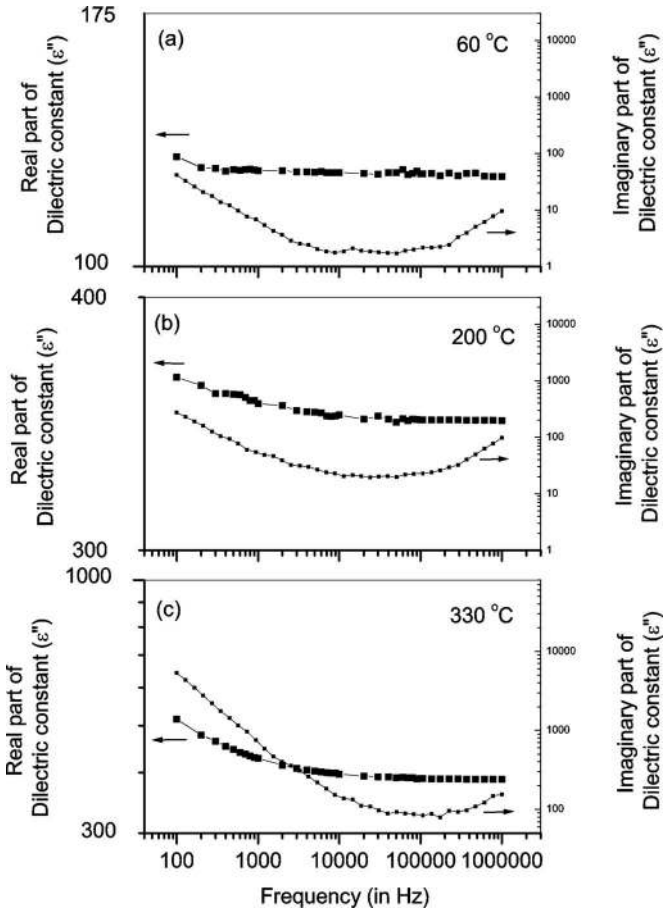

FIG. 5. (a), (b), and (c) represent the dielectric responses at 60, 200, and 330 °C, respectively. The responses at low temperature resemble the Maxwell-Wagner-type dielectric response, whereas at high temperature, hopping charge carriers predominate.

charge in dielectric solid occurs by defect formation. Therefore defects in solids can change its true dielectric characteristics by many aspects and they can change the dielectric response of solids, too. Hence, it can be suspected that hopping charge in the sample can change its dielectric response. According to earlier reports,[29,30] a strong low frequency dispersion can be recognized as long range hopping and from the dielectric response of PZ (Figs. 3–5), it seems that the present samples are affected by long range hopping.

C. ac conductivity and Arrhenius plot

In Fig. 6(a), ac conductivity of PZ thin film has been presented in log-log scale. The ac conductivity is calculated from the equation

$$\sigma_{ac} = 2\pi f \varepsilon_0 \varepsilon' \tan\delta = 2\pi f \varepsilon''. \tag{2}$$

Here, σ_{ac} stands for ac conductivity and ε_0 stands for permittivity of free space. f, ε', and ε'' are defined as frequency, real part of the dielectric constant, and imaginary part of the dielectric constant, respectively. From this figure, it has been noticed that at the low frequency region, ac conductivity has relatively lesser frequency dependence than at high frequency region. The frequency dependence has been measured by their slopes at different frequency regions. It is well known that ac conductivity of dielectric materials depends

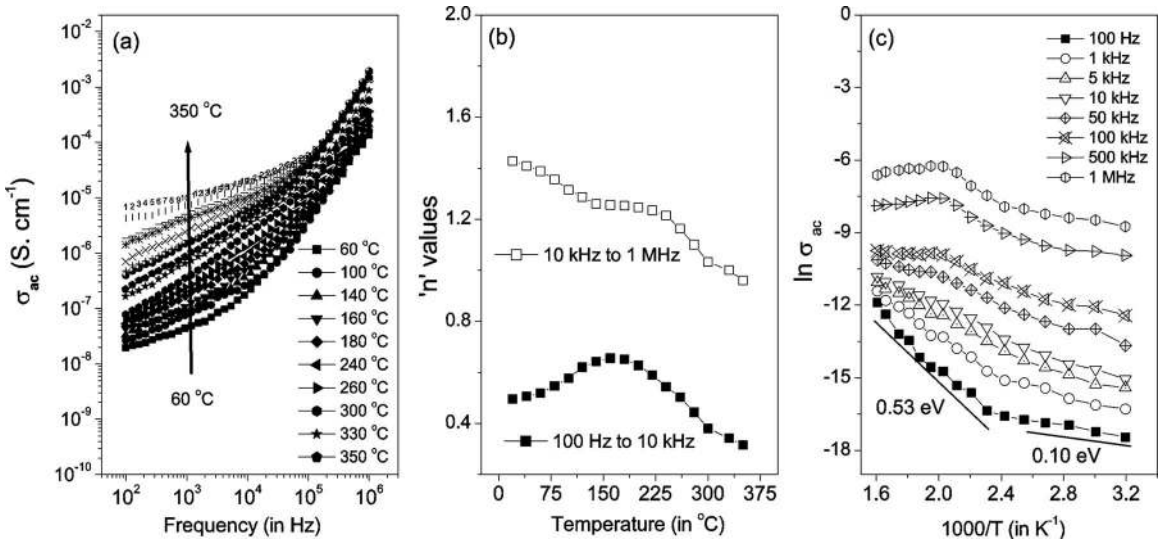

FIG. 6. (a) ac conductivities at various temperatures show that the frequency dependency on it decreases with increasing temperature. (b) Temperature dependency of n values shows that at the low frequency region (100 Hz–10 kHz), there is an initial increase in values followed by an expected decreasing nature on increasing temperature (above 160 °C), whereas at the high frequency region (10 kHz–1 MHz), the increasing correlation between trapped charges shows a decreasing trend of these values on increasing temperature. (c) Arrhenius plots at various frequencies confirm the presence of hopping charge due to oxygen vacancies in PZ.

on "many body interaction" of trapped charges and a relation is presented by a power law[31] given by

$$\sigma_{ac} = A\omega^n, \tag{3}$$

where $\omega = 2\pi f$ and n is a function of temperature and the measure of frequency dependence of ac conductivity. A is a constant at a particular temperature. Figure 6(b) shows the dependency of n on temperature. It has been noticed that at the high frequency region, the n values are near the value of 2. This indicates the ω^2 dependency of ac conductivity. In general, n values lie between the values of 0 and 1.[32] In the present study, the samples show that in the low frequency region, the n values are within 0 and 1 and at the high frequency region, the values tend to reach 2. According to parallel G-C combination with resistance in series, ac conduction process shows ω^2 dependency[16] and for this kind of system, dc conduction path is present down to zero frequency. The convenient parameter is effective conductivity $\sigma(\omega)$, together with the real part of the dielectric constant, $\varepsilon'(\omega)$. The expressions are presented in the limit of small series resistance as follows:

$$\sigma(\omega) = \sigma_0 \frac{1 + \omega^2\tau^2/b}{1 + \omega^2\tau^2}, \tag{4}$$

$$b = R_0 G_0 \ll 1,$$

$$\tau = R_0 C_0,$$

$$\varepsilon'(\omega) = \varepsilon_0 \frac{1}{1 + \omega^2\tau^2}. \tag{5}$$

Here, σ_0 is the dc conductivity of the sample, R_0 is the series resistance, G_0 is the dc conductance, C_0 is the capacitance of the sample at zero frequency, and τ is defined as the relaxation time of the sample. According to expressions (4) and (5), the imaginary part of the dielectric constant should be frequency dependent at the entire frequency region by the following relation:

$$\varepsilon''(\omega) \simeq \varepsilon_0 \omega\tau/(1 + \omega^2\tau^2). \tag{6}$$

However, according to relations (4)–(6), a loss peak in $\varepsilon''(\omega)$ should correspond to a region of $\sigma(\omega) \propto \omega^2$ followed by a saturation value of conductance.[16] The present frequency range of measurement shows that at the high frequency region, n values of Eq. (3) tend to 2 and it has never reached 2 or its saturation value [Fig. 6(a)]. As the dielectric loss peak and saturation value of ac conductivity have never been seen within the frequency and temperature ranges of measurement, it can be stated that the dielectric response of PZ thins film has been measured below the loss peak frequency all throughout the temperature and frequency ranges. Moreover the equivalent circuit with parallel G-C combined with series resistance should have a strong dispersion of loss at the low frequency region with $\varepsilon''(\omega)$ proportional to $1/\omega$.[16] This strong dispersion corresponds to the dc conduction, while ε' remains independent of frequency until the loss peak frequency. However, in the present report, a clear drop of the real part of the dielectric constant has been observed at the lower frequency region without any loss peak [Fig. 4(a)]. This drop is due to hopping charge dominated mechanism that took part in the low frequency region (already mentioned in Sec. III B). These hopping charges mostly come from the defect states due to oxygen vacancies in bulk or in interfacial regions.

The observed n values are within 0 and 1 at the low frequency region (100 Hz–10 kHz), whereas at the high frequency region (10 kHz–1 MHz), n values lie between 1 and 2. According to these two different n values [Fig. 6(b)] or two different regions of ac conductivity [Fig. 6(a)], it can be assumed that there must be two different mechanisms playing a role in the dielectric response of PZ thin films. Moreover, from Fig. 6(b), it has been observed that the tempera-

ture dependent n values are also different for different frequency regions. In the low frequency region, it has been noticed that there is an initial rising of n values on increasing temperature up to 160 °C followed by a subsequent decrease in those values. In the case of the high frequency region, a steady decrease in n values has been observed. However, these two different natures of n values in the two different frequency regions are further indication of two different mechanisms taking part in the dielectric response of the thin films under study.

It is well known that the temperature dependence of n values defines the correlation of potential wells present in a many body system.[33] The interaction between all dipoles participating in the polarization process is characterized by this parameter and the increase in n values indicates the increase in correlation. The fact of ac field assisted hopping charge can be visualized by the trapped charge carriers in separate potential wells and they are able to hop on one potential well to another potential well on application of ac field. In a crystalline material, such potential wells are separated by energy barriers with varied heights and thus the hopping probabilities from one potential well to another have their own individual time constants. For the higher energy barriers, time constants will be greater than for the lower energy barriers. Hence, the probability of hopping will be decreased for a potential pair separated by a higher energy barrier. However, greater time constants or lesser hopping probabilities signify the lower frequency of hopping from one potential well to another. Therefore, the potential wells separated by higher energy barriers will respond, at the lower frequency region, whereas defect sites involving lower distortions in lattice will create a small energy barrier and will respond at the higher frequency region. Thus, the extent of hopping is measured by ac conductivity because it reveals the ac field assisted hopping mechanism. Furthermore, according to the Maxwell-Boltzmann distribution, we can say that the number of traps with a lower energy barrier is higher in number in comparison to long range hopping. So the short range hopping response should be observed in the high frequency region and the more number of short range traps should lead to increase the ac conductivity in this region. In addition, according to the same distribution, at the higher temperatures, energy distributions of traps should become uniform by minimizing the frequency dependence of ac conductivity. However, from Fig. 6(a) it has been noticed that ac conductivity of PZ thin film is higher at the high frequency region and the frequency dependence of ac conductivity has been minimized at higher temperatures. Therefore, it can be predicted that trapped charges obeys the Maxwell-Boltzmann distribution. However, from the above discussions, we have come to know that the increase in ac conductivity depends on correlation of potential well of trap sites and the number of probable trap sites (with a particular time constant) taking part in ac conductivity. Hence there may be two possibilities to increase temperature dependent n values at the low frequency region:

(i) the weakly correlated systems may become strongly correlated systems with the increase in temperature and
(ii) the number of traps with weakly correlated systems is being increased with increasing temperature, giving rise to probability of ac field assisted hopping at higher frequencies.

The assumption of weakly correlated systems getting strongly correlated systems on increasing temperature leads to visualize that with the increase in temperature, trapped charges are being more trapped in their corresponding potential wells. However, according to this assumption, with increasing temperature, trapped charges would have not taken part in the ac conduction or probably they would have responded at a very low frequency. Thus at the same frequency region, there would be diminution of n values on increasing temperature, whereas the present study shows that there is an increase in n values with increasing temperature [Fig. 6(b)]. So the first possibility lacks the explanation of the increase in n values with increase in temperature. On the other hand, with a decrease in potential barrier height with an increase in temperature, the long range hopping can act as a short range hopping. However, it can be assumed that the conversion probability from long range hopping to short range hopping is different for each potential well pair. So with the increase in temperature, attribution of converted short range hopping to existing short range hopping can exhibit a sudden increase in ac conductivity at relatively higher frequencies. However, the sudden enhancement in ac conductivity towards higher frequencies can increase the slope of ac conductivity within a fixed frequency range. Thus within a fixed frequency region, increase in n values with increasing temperature is possible. Moreover, from the steady decrease of n values after 160 °C [Fig. 6(b)], it can be presumed that after 160 °C, very few conversions took place to exhibit steep rising of ac conductivity or there must be no more long range hopping traps to convert into short range hopping traps. As we know that the increase in probability of field assisted hopping charge is the manifestation of increasing ac conductivity, the increase in number of weakly correlated systems must be the reason to increase n values below the temperature of 160 °C. Hence, among the possibilities to increase the n values, the second possibility is more acceptable than the first one.

Being the measure of hopping of charge carriers from one trap site to another, ac conductivity at the low frequency region is the signature of relatively long range hopping probability, while in the higher frequency, relatively short rang hopping leads to conduction.[33] However, at a particular frequency, the ac field assisted hopping probability can be measured by the Arrhenius plot (Fig. 6) and it can be seen that the hopping probability is different at different temperatures. According to Fig. 6, two distinct regions of ac conductivity have been noticed with respect to temperature. It has been noticed that ac conductivity at 100 Hz has an activation energy of 0.10 eV within a temperature range of room temperature to 160 °C, whereas the value becomes 0.53 eV within the range of 160–350 °C. However, these small values of activation energy of ac conductivity have been attributed to the shallow trap controlled current conduction of the

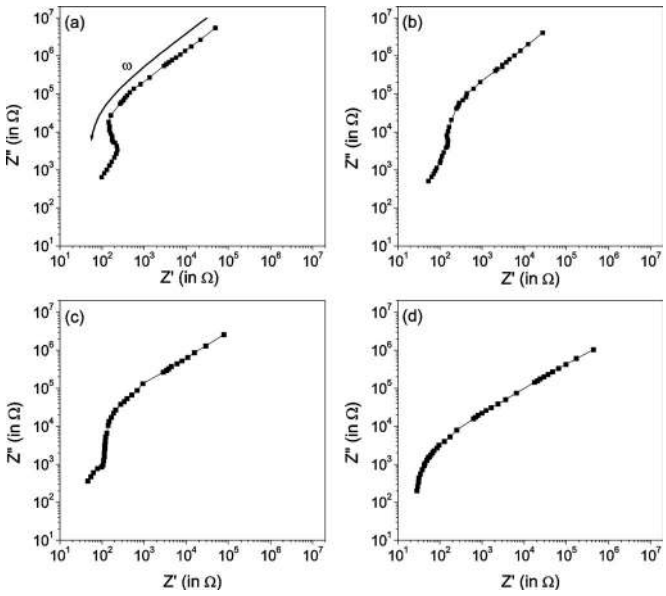

FIG. 7. Nyquist plots at various temperatures. (a), (b), (c), and (d) stand for temperatures of 60, 120, 180, and 350 °C, respectively. Up to 180 °C, the presence of two different responses is prominent and above that, only one response dominates, e.g., the Nyquist plot at 350 °C. ω with the arrow sign shows that the higher frequency region is towards the origin, which is true for all the four plots, (a)-(d).

sample[31] because the band gap of PZ ceramic is as high as 3.93 eV.[34] The shallow trapped controlled conduction is created from the donor states as a possible consequence of oxygen vacancies, as

$$O_0 = \tfrac{1}{2}O_2 + V_{\ddot{O}} + 2e', \tag{7}$$

where O_0 represents an oxygen ion situated at the oxygen site of a perovskite crystal, and $V_{\ddot{O}}$ means an oxygen vacancy, which liberates two (almost) free electrons (denoted by e') very near the conduction band. In the Arrhenius plot (Fig. 6), the steep rising in ac conductivity after 160 °C indicates that the charge carriers of different regions, namely, interior grains, have started their influence over grain boundaries.[33] However, with the increase in frequency, the two temperature regions slowly become indistinguishable. This slow change has been seen up to 10 kHz, whereas from 100 kHz and above 220 °C, an almost flat region has been observed [Fig. 6(c)]. This region probably corresponds to saturation in the number of liberated electrons from the donor states.[33]

D. Nyquist plots

Z'' versus Z' plots in log-log scale, widely known as the Nyquist plot,[35] have been presented at four different temperatures (60, 120, 180, and 350 °C, respectively) in Figs. 7(a)–7(d). The two distinguished regions in the Nyquist plots at 60, 120, and 180 °C [Figs. 7(a)–7(c)] indicate that at these temperatures, there must be the combination of two equivalent circuits for impedance response of the sample. From the Nyquist plot at 350 °C [Fig. 7(d)], it has been observed that at a very high temperature, only one equivalent circuit dominates for impedance response. It has been seen from dielectric dispersion that at a low frequency, long range hopping charge carriers dominate the system and the hopping charge dominated response extends to the high frequency region with increasing temperature (Fig. 4). Therefore hopping charge dominated equivalent circuit is expected at high temperature. From Fig. 7, it has been seen that Z' at 1 MHz is a decreasing function of temperature and the values of Z' at 1 MHz are 98, 52, 45, and 28 Ω at 60, 120, 180, and 350 °C, respectively. At 100 Hz a decrease in Z' values has been observed up to 120 °C followed by an increasing trend with increase in temperature (at 100 Hz, $Z'=49$, 27.5, 78.8, and 433 kΩ at 60, 120, 180, and 350 °C, respectively). Therefore, it seems that the PZ thin film gives a signature of negative temperature coefficient of resistivity (NTCR) at high frequency, whereas NTCR effects normally come from grain contributions.[36,37] Moreover, Z' values at the low frequency region lack NTCR at high temperatures (at above 120 °C) and show a positive temperature coefficient of resistivity (PTCR). According to Sinclair and West,[38] grain boundary effect is responsible for PTCR. Hence, at high temperature, Z' response is dominated by grain boundary effect.

From the above discussion it is obvious that there must be a combination of two different equivalent circuits to explain the impedance response of the film under study. However, the investigation of equivalent circuits for the impedance response reveals that the assumption of two series *R-C* circuits in series or any other two combinations of *R-C* circuits is unable to explain the ω^2 dependency of ac conductivity. So it is obvious that there must be a *G-C* circuit contribution. Among the various combinations, the series combination of parallel *G-C* circuit and series *R-C* circuit is found to be suitable for the response. According to the ω^2 dependency of ac conductivity, *G-C* circuit dominated impedance response is obvious at the high frequency region, whereas at the low frequency region, series *R-C* circuit dominated response can be justified. However, for series *R-C* circuit, effective impedance can be written as

$$Z_{R\text{-}C} = R_1 + \frac{1}{j\omega C_1}. \tag{8}$$

Similarly, the effective impedance of the *G-C* circuit can be presented as

$$Z_{G\text{-}C} = \frac{1}{G}\left(\frac{1 - j\omega C_2/G}{1 + \omega^2 C_2^2/G^2}\right) = \frac{1}{G(1+\omega^2\tau_2^2)} - j\frac{\omega\tau_2}{1+\omega^2\tau_2^2}, \tag{9}$$

where $\tau_2 = C_2/G$.

Then the effective impedance of the total circuit should be

$$\begin{aligned} Z_{\text{eff}} &= Z_{R\text{-}C} + Z_{G\text{-}C} \\ &= R_1 + \frac{1}{j\omega C_1} + \frac{1}{G(1+\omega^2\tau_2^2)} - j\frac{\omega\tau_2}{1+\omega^2\tau_2^2} \\ &= \left(R_1 + \frac{1}{G(1+\omega^2\tau_2^2)}\right) - j\left(\frac{1}{\omega C_1} + \frac{\omega\tau_2}{1+\omega^2\tau_2^2}\right) \\ &= Z' - jZ''. \end{aligned} \tag{10}$$

From Eq. (10), we can say that

$$Z' = \left(R_1 + \frac{1}{G(1+\omega^2\tau_2^2)}\right) \quad \text{and} \quad Z'' = \left(\frac{1}{\omega C_1} + \frac{\omega\tau_2}{1+\omega^2\tau_2^2}\right). \tag{11}$$

From the concept of the *R-C* and *G-C* circuits, we know that G is an increasing function of frequency, whereas resistance should be independent of it. Hence, from Eq. (11) it is obvious that Z' is a decreasing function of frequency. On the other hand, from the same equation, it can also be suggested that Z'' is a decreasing function of frequency, too. From the equation of Z'' and the frequency dispersion of the real part of the dielectric function [Fig. 4(a)], it can be interpreted that C_1 is independent of frequency or a very slowly decreasing function of it. Hence, $1/\omega C_1$ should be a decreasing function of frequency. Furthermore, $\omega\tau_2$ is greater than 2π because $1/f$ is greater than τ_2 and $\omega=2\pi f$ [Eqn. (2)]. It should be noted that τ_2 signifies the time constant of the *G-C* circuit and as there is no loss peak observed at the high frequency region, $1/f$ is greater than τ_2. Therefore, $\omega\tau_2/(1+\omega^2\tau_2^2)$ is a decreasing function of frequency as $\omega\tau_2 > 2\pi$ and thus $\omega\tau_2 > 1$. However, it can be clearly seen in Fig. 7 that on increasing frequency, the Z'' is decreasing and tending towards the origin. However, the analytical investigations of the functions show that according to partial differentiation,

$$\left(\frac{\partial Z'}{\partial \omega}\right)_T = -\frac{1}{G^2(1+\omega^2\tau_2^2)^2}\{G'(\omega) + 2\omega\tau_2^2\} < 0. \tag{12}$$

Here $G'(\omega)=(\partial G/\partial\omega)_T$ and it is an increasing function as σ_{ac} is the increasing function of frequency [Fig. 6(a)]. Therefore, $G'(\omega)>0$. Moreover, as the rest of the parameters in the Eq. (12) are positive, Z' is a decreasing function of frequency. However, it has been seen that on increasing frequency Z' values decrease towards origin in Fig. 7. Similarly

$$\left(\frac{\partial Z''}{\partial \omega}\right)_T = -\frac{1}{\omega^2 C_1^2}\{\omega C_1'(\omega) + C_1\} + \frac{\tau_2}{(1+\omega^2\tau_2^2)^2} - \frac{\omega^2\tau_2^3}{(1+\omega^2\tau_2^2)^2}. \tag{13}$$

Here $C_1'(\omega)=(\partial C_1/\partial\omega)_T$ and from the Eq. (13) we can say that the nature of Z'' with respect to ω depends on C_1', ω and τ_2. However, as τ_2 is less than 1 μs ($1/f > \tau_2$ and in the present experiment a maximum value of $f=10^6$Hz) and as $\omega\tau_2 > 2\pi$, $\omega^2\tau_2^3/(1+\omega^2\tau_2^2)^2 > \tau_2/(1+\omega^2\tau_2^2)^2$. Therefore, $(\partial Z''/\partial\omega)_T < 0$. Thus, it is analytically justified that Z'' is a decreasing function of frequency.

From the previous discussion, it is obvious that with increase in temperature, there will be an increase in G values [or σ_{ac} values from Fig. 6(a)]. Hence, there will be a decrease in Z' values (Eq. (11)). Howevers the prediction is not fully supported by the partial differentiation of Z':

$$\left(\frac{\partial Z'}{\partial T}\right)_\omega = \left(\frac{\partial R_1}{\partial T}\right)_\omega - \frac{1}{G^2(1+\omega^2\tau_2^2)^2}\{G'(T) + 2G\omega^2\tau_2\tau_2'(T) + \omega^2\tau_2^2 G'(T)\}. \tag{14}$$

In this equation, $(\partial R_1/\partial T)_\omega$ can be positive and negative. Moreover, at the low frequency region, the rest part of the right hand side can be neglected as at this region, $G'(T) \equiv (\partial G/\partial T)_\omega$ is very low [Fig. 6(a)]. On the other hand, the contribution of τ_2 is not valid the at low frequency region as the low frequency response is *R-C* circuit dominated and ac conductivity does not show any ω^2 dependency. The validity of τ_2 should be taken into account at the *G-C* circuit dominated response. Hence, the PTCR nature of R_1 can make Z' an increasing function of temperature because for the PTCR nature of R_1, $(\partial R_1/\partial T)_\omega > 0$. From the earlier discussion, it has been noticed that at high frequency, Z' is a decreasing function of temperature and at low frequency, there is an initial drop in Z' value followed by an increasing trend with temperature (according to noted values at the beginning of this section). Therefore, at the low frequency region, R_1 has NTCR effect on Z', whereas on increasing temperature, R_1 has its PTCR effect on it. As it is well known that on increasing temperature, the charge carriers of different regions, namely, interior grains, have started their influence over grain boundaries,[33] the PTCR effect of R_1 is due to the effect of increasing trapped charge density on increasing temperature. It has been already reported that the PTCR effect comes from the grain boundaries[38] and grains do not show the PTCR effect.[36,37] In the present study of PZ thin films, it has been seen that the NTCR of R_1 has become PTCR on increasing temperature. If the response would have been from grain boundaries, there might have been only PTCR effect all throughout the temperature range. Therefore, the conversion of NTCR of R_1 to PTCR on increasing temperature indicates the influence of trapped charge only on R_1 and the impedance response is from grains only. Thus the PTCR effect on Z' is not from the grain boundaries. On the other hand, at high frequency region lesser influence of trapped charge and the dominance of *G-C* circuit make Z' a purely decreasing function of temperature [Fig. 7]. Furthermore, the observation of the slow absence of high frequency response (response near the origin) in Nyquist plots on increasing temperature [Fig. 7] is one of the justifications of the decreasing nature of $\tau_2'(T)$. Another justification can be seen from the Fig. 4(b) as on increasing temperature, the increasing nature of the imaginary part of the dielectric constant has shifted towards the higher frequencies. As the decreasing nature of $\tau_2'(T)$ signifies that $\tau_2'(T) < 0$, according to Eq. (14), $(\partial Z'/\partial T)_\omega$ could have been positive at the high frequency region. However the impedance response at the high frequency region shows that $(\partial Z'/\partial T)_\omega$ is negative as on increasing temperature, Z' is a decreasing function (Fig. 7 and mentioned values at the beginning of this section). Therefore, the influence of $\tau_2'(T)$ on $G'(T)$ is negligible at higher frequency to make the entire value of $G'(T)+2G\omega^2\tau_2\tau_2'(T) + \omega^2\tau_2^2 G'(T)$ negative.

The analytical insight from the partial differentiation of Z'' shows:

$$\left(\frac{\partial Z''}{\partial T}\right)_\omega = -\frac{C_1'(T)}{\omega C_1^2} + \frac{\omega\tau_2'(T)}{(1+\omega^2\tau_2^2)} - \frac{\omega^3\tau_2^2\tau_2'(T)}{(1+\omega^2\tau_2^2)^2} = -\frac{C_1'(T)}{\omega C_1^2} + \frac{\omega\tau_2'(T)}{(1+\omega^2\tau_2^2)^2}. \tag{15}$$

From the Eq. (15) it is obvious that the Z'' can be either a

decreasing or an increasing function of temperature. From the behavior of dielectric dispersion (Figs. 3 and 4), we can say that below the phase transition temperature, $C_1^{/}(T)=(\partial C_1/\partial T)_\omega>0$, but above the phase transition temperature, $C_1^{/}(T)<0$, whereas another parameter is $\tau_2^{/}(T)=(\partial\tau_2/\partial T)_\omega<0$. Therefore, there are two possibilities, either Z'' can be an increasing function or a decreasing function depending on the phase transition temperature. However, from Fig. 7 it has been seen that, in the present study, Z'' is a decreasing function of temperature irrespective of frequency. At 100 Hz, Z'' values are 5.42, 4.04, 2.57 and 1.05 MΩ at the temperatures of 60, 120, 180, and 350 °C, respectively, whereas the some trend has also been seen at 1 MHz and for the same temperatures and the Z'' values are 645, 510, 362, and 202 Ω respectively. This phenomenon indicates that above the phase transition temperature, there is a strong influence of $\omega\tau_2^{/}(T)/(1+\omega^2\tau_2^2)^2$ over $-C_1^{/}(T)/\omega C_1^2$ to make Z'' a decreasing function of temperature.

However, instead of *R-C* in series with *G-C* parallel, if the choice of the equivalent circuit would have been the combination of parallel *R-C* circuit with parallel *G-C* circuit, Eq. (11) would have been as follows:

$$Z'=\left(\frac{1}{R_1}+\frac{1}{G(1+\omega^2\tau_2^2)}\right)\quad\text{and}\quad Z''=\left(\omega C_1-\frac{\omega\tau_2}{1+\omega^2\tau_2^2}\right). \tag{16}$$

According to Eq. (16),

$$\left(\frac{\partial Z'}{\partial T}\right)_\omega=-\frac{R_1^{/}(T)}{R_1^2}-\frac{1}{G^2(1+\omega^2\tau_2^2)^2}\{G^{/}(T)+2G\omega^2\tau_2\tau_2^{/}(T)+\omega^2\tau_2^2G^{/}(T)\}, \tag{17}$$

where $R_1^{/}(T)=(\partial R_1/\partial T)_\omega$. From the above equation, it is clear that at low frequency region, the negative value of $(\partial Z'/\partial T)_\omega$ (initial drop of Z' at low temperatures) can only be explained when $R_1^{/}(T)=(\partial R_1/\partial T)_\omega>0$. On the other hand, at the same frequency region, $R_1^{/}(T)=(\partial R_1/\partial T)_\omega<0$ can only explain the positive value of $(\partial Z'/\partial T)_\omega$ (the increasing nature of Z' at high temperatures). This phenomenon signifies that at low frequency, the temperature coefficient of R_1 is temperature dependent. However, to explain the decreasing nature of $(\partial Z'/\partial T)_\omega$, $[1/G^2(1+\omega^2\tau_2^2)^2]\{G^{/}(T)+2G\omega^2\tau_2\tau_2^{/}(T)+\omega^2\tau_2^2G'(T)\}$ has to be positive with the influence over $R_1^{/}(T)$. Though there can be an explanation for the decreasing nature of $(\partial Z'/\partial T)_\omega$, the combination of equivalent circuits of parallel *R-C* and *G-C* fails to explain the decreasing nature of $(\partial Z''/\partial T)_\omega$.

From the Eq. (16), it can be derived that

$$\left(\frac{\partial Z''}{\partial T}\right)_\omega=\omega C_1^{/}(T)-\frac{\omega\tau_2^{/}(T)}{(1+\omega^2\tau_2^2)^2}. \tag{18}$$

$C_1^{/}(T)$ is an increasing function of temperature before the phase transition temperature and as $\tau_2^{/}(T)$ is a decreasing function of temperature, $C_1^{/}(T)>0$ (below phase transition) and $\tau_2^{/}(T)<0$. Hence below the phase transition temperature (~235 °C),$(\partial Z''/\partial T)_\omega$ should always be positive, which is not observed in the present experiment. It has been observed that Z'' is a decreasing function of temperature irrespective of frequency and thus $(\partial Z''/\partial T)_\omega$ is always negative. Though the negative values of $C_1^{/}(T)$ above the phase transition can explain the decreasing nature Z'' with respect to temperature [assuming $|C_1^{/}(T)|>|\tau_2^{/}(T)|$], the decreasing nature of Z'' below the phase transition temperature of PZ cannot be explained by the parallel *R-C* circuit contribution. Therefore, we found that equivalent circuit consisting of *R-C* in series with *G-C* parallel is the better choice to explain the dielectric as well as impedance response of the films.

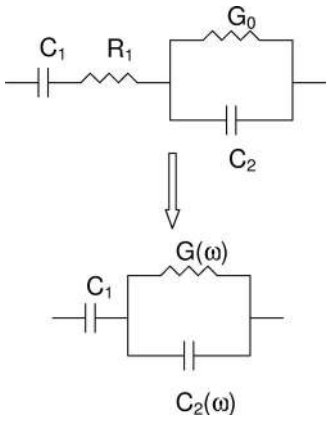

FIG. 8. Equivalent circuit that most likely resembles the dielectric response of the thin films under study.

To formulate the dielectric property of the proposed equivalent circuit, drawn in Fig. 8, it can be assumed that the capacitance is in series with the parallel *G-C* circuit. According to this assumption or simplification of the circuit, it can be written that

$$\varepsilon(\omega)\simeq C_1\frac{1+j\omega\tau'}{1+j\omega\tau' r}=C_1\frac{1+r\omega^2\tau'^2-j\omega\tau' r}{1-r^2\omega^2\tau'^2}$$
$$=C_1\frac{1+r\omega^2\tau'^2}{1-r^2\omega^2\tau'^2}-j\frac{\omega\tau' r}{1-r^2\omega^2\tau'^2}=\varepsilon'(\omega)-j\varepsilon''(\omega). \tag{19}$$

Here in the Eq. (19), $r=C_1/C_2$ and $1/r\tau'=G(\omega)/C_1$. According to Eq. (19), $\varepsilon'(\omega)$ should be almost frequency independent and $\varepsilon''(\omega)$ is an increasing function of frequency. In the present study of dielectric dispersion, we have seen that the real part of the dielectric constant is almost independent of frequency at low low temperature region [Fig. 4(a)]. The extension of dielectric dispersion with frequency at the high temperature region is the manifestation of hopping charges present in the system. As the long range hopping charges responsed in the low frequency region,[27] these hopping charge conduction at low frequency region can give rise to G_0. According to the explanation in section C and according to the $G(\omega)$-$C(\omega)$ circuit, at the low frequency region, ε'' should follow the G_0/ω relation. Therefore at the low frequency region, conductance component dominated dielectric response is expected. The initial decreasing nature of ε'' with increasing ω or frequency (Figs. 4 and 5) is the signature of its conductance component dominated response it and thus it supports the suggested equivalent circuit.

IV. CONCLUSIONS

In the present study, we have characterized $(110)_t$ preferred oriented PZ thin films grown on $Pt(111)/Ti/SiO_2/Si$. The growth mechanism has been explained by means of probable Pt_3P alloy formation and justified with lattice mismatch. Slim *P-E* hysteresis loop has been explained by $(110)_t$ preferred orientation of PZ films and it has been compared to earlier reported data. In addition, it has been explained from the thickness point of view as well as from crystallographic orientation. Dielectric response of PZ thin films has been explained by the charge tarps and the domination of these charge traps at the low frequency region. Dielectric dispersion of the films has exhibited Maxwell-Wagner-type dispersion, but the nature of ac conductivity excludes the possibility. Further study of Nyquist plot in log-log scale has revealed the true equivalent circuit to explain the dielectric dispersion and it has been justified that the equivalent circuit is a combination of series *R-C* and parallel *G-C* circuits. Here in this paper, we have explained that the temperature dependent *n* values of power law are not only the signature of correlation of potential wells of trapped charge but also the indication of temperature dependent "potential well pair" populations. Therefore, the dielectric property of the films is not usual; rather it is anomalous by nature.

[1]M. H. Francombe, Thin Solid Films **13**, 413 (1972).
[2]D. L. Polla and L. F. Francis, MRS Bull. **21**, 59 (1996).
[3]A. S. Mischenko, Q. Zhang, J. F. Scott, R. W. Whatmore, and N. D. Mathur, Science **1**, 1271 (2006).
[4]G. Shirane, E. Swaguchi, and Y. Takagi, Phys. Rev. **84**, 476 (1951).
[5]B. Xu, Y. Ye, and L. E. Cross, J. Appl. Phys. **87**, 2507 (2000).
[6]R. A. Wolf and S. Troiler-McKinstry, J. Appl. Phys. **95**, 1397 (2004).
[7]Q. M. Zhang, S. J. Jang, and L. E. Cross, J. Appl. Phys. **65**, 2807 (1989).
[8]N. J. Donnelly, G. Catalan, C. Morros, R. M. Bowman, and J. M. Gregg, J. Appl. Phys. **93**, 9924 (2003).
[9]W. Y. Pan, Q. M. Zhang, A. Bhalla, and L. E. Cross, J. Am. Ceram. Soc. **72**, 571 (1989).
[10]P. Yang and D. A. Pyne, J. Appl. Phys. **71**, 1361 (1992).
[11]E. Sawaguchi, H. Maniwa, and S. Hoshini, Phys. Rev. **83**, 10 78 (1951).
[12]F. Jona, G. Shirane, F. Mazzi, and R. Pepinsky, Phys. Rev. **105**, 849 (1957).
[13]T. Tani, J.-F. Li, D. Viehland, and D. A. Payne, J. Appl. Phys. **75**, 3017 (1994).
[14]J. Zhai, Y. Yao, X. Li, T. F. Hung, Z. K. Xu, H. Chen, E. V. Colla, and T. B. Wu, J. Appl. Phys. **92**, 3990 (2002).
[15]E. M. Alkoy, S. Alkoy, and T. Shioski, Jpn. J. Appl. Phys., Part 1 **44**, 8606 (2005).
[16]A. K. Jonscher, *Dielectric Relaxation in Solids* (Chelsea Dielectric, London, 1983).
[17]J. Parui and S. B. Krupanidhi, J. Appl. Phys. **100**, 044102 (2006).
[18]S. Y. Chen and I. W. Chen, J. Am. Ceram. Soc. **77**, 2332 (1994).
[19]Z. Huang, Q. Zhang, and R. W. Whatmore, J. Appl. Phys. **85**, 7355 (1999).
[20]L. Shebanov, M. Kusnetsov, and A. Sternberg, J. Appl. Phys. **76**, 4301 (1994).
[21]G. Shirane and S. Hoshino, Acta Crystallogr. **7**, 203 (1954).
[22]O. E. Fesenko, R. V. Kolesova, and Yu. G. Sindeyev, Ferroelectrics **20**, 177 (1978).
[23]X. G. Tang, J. Wang, X. X. Wang, and H. L. W. Chan, Solid State Commun. **130**, 373 (2004).
[24]S. Chattopadhyay, P. Ayyub, V. R. Pakar, M. S. Muttani, S. P. Pai, S. C. Purandare, and R. Pinto, J. Appl. Phys. **83**, 7808 (1998).
[25]I. Kanno, S. Hayashi, M. Kitagawa, R. Takayama, and T. Hirao, Appl. Phys. Lett. **66**, 145 (1995).
[26]M. Pollak and T. H. Geballe, Phys. Rev. **122**, 1742 (1961).
[27]A. Mansingh, Bull. Mater. Sci. **2**, 325 (1980).
[28]R. Lovell, J. Phys. C **7**, 4378 (1974).
[29]P. Doerenbos, H. W. den Haetog, R. Kruizinga, and S. Vrind, Phys. Rev. B **35**, 5774 (1987).
[30]X. Chen, A. I. Kington, L. Mantase, O. Auciello, and K. Y. Hsieh, Integr. Ferroelectr. **3**, 355 (1993).
[31]S. S. N. Bharadwaja and S. B. Krupanidhi, Thin Solid Films **391**, 126 (2001).
[32]S. S. N. Bharadwaja, P. Victor, P. Venkateswarulu, and S. B. Krupanidhi, Phys. Rev. B **65**, 174106 (2002).
[33]S. Bhattacharyya, S. S. N. Bharadwaja, and S. B. Krupanidhi, J. Appl. Phys. **88**, 4294 (2000).
[34]V. I. Zametin, Phys. Status Solidi B **124**, 625 (1984).
[35]J. Liu, C.-G. Duan, W.-G. Yin, W. N. Mei, R. W. Smith, and J. R. Hardy, Phys. Rev. B **70**, 144106 (2004).
[36]I. Ueda and K. Ikegami, J. Phys. Soc. Jpn. **20**, 546 (1965).
[37]M. Kuwubara, S. Suemura, and M. Kawahara, Am. Ceram. Soc. Bull. **64**, 1394 (1985).
[38]D. C. Sinclair and A. R. West, J. Appl. Phys. **66**, 3850 (1989).